

Ignition and combustion characteristics of the gas turbine slinger combustor

Seongman Choi^{1,*}, Donghun Lee² and Jeongbae Park³

¹*Division of Mechanical and Aerospace System Engineering, Chonbuk National University, 664-14, Deokjin Dong 1 Ga, Jeonju City, Chonbuk, 561-756, Korea*

²*Power Systems R&D Center, Samsung Techwin Co., LTD., Sungju Dong 28, Changwon City, Gyeongnam, 641-717, Korea*

³*Agency for Defense Development, Yuseong, Daejeon, Korea*

(Manuscript Received June 4, 2007; Revised November 9, 2007; Accepted November 12, 2007)

Abstract

This paper describes the ignition and combustion characteristics of a gas turbine slinger combustor with rotating fuel injection system. An ignition test was performed under various airflow, temperature and pressure conditions with fuel nozzle rotational speed. From the test, there are two major factors influencing the ignition limits: the rotational speed of the fuel nozzle, and the mass flow parameter. Better ignition capability could be attained through increasing the rotational speed and air mass flow. From the spray visualization and drop size measurement, it was verified that there is a strong correlation between ignition performance and drop size distribution. Also, we performed a combustion test to determine the effects of rotational speed by measuring gas temperature and emission. The combustion efficiency was smoothly enhanced from 99% to 99.6% with increasing rotational speed. The measured pattern factor was 15% and profile factor was 3%.

Keywords: Slinger combustor; Rotating fuel injection system; Ignition; Combustion

1. Introduction

An annular combustor with rotating fuel injection system, what is called a slinger combustor, has been frequently employed in gas turbines. Such a system is successfully adopted in a number of engines of Turbomeca and others. The main advantages of this system are its cheapness and simplicity. In terms of atomization, a rotating fuel injection system makes a fine fuel spray even at part load or idle conditions. [1] The role of a gas turbine fuel atomizer is to distribute the drops into the combustion zone. The spatial distribution depends on the penetration of fuel spray into the primary zone and is closely coupled to the aerodynamic flow pattern. A pressure swirl atomizer or air-blast atomizer can meet these requirements. But in

general, these injectors require high manufacturing and design quality for their components such as a swirl chamber and orifice. The rotating fuel injection system can be applied economically to the gas turbine combustor. [2]

Yet, in spite of its simplicity, the detailed ignition and combustion characteristics of the slinger combustor were for a long time not fully understood. [3-4]

Maskey and Marsh [3] briefly explained about the slinger combustor characteristics in terms of engine operating conditions by using a J69-T-25 turbo jet engine; but they did not show combustor rig test results. Rogo and Trauth [4] explained the slinger combustor in terms of engine scale design by using a YJ402-CA-400 turbojet engine. By using empirical correlation of droplet size, which was obtained from a simplex pressure atomizing nozzle, they explained combustion characteristics with droplet size. These previous results could not provide details of ignition

*Corresponding author. Tel.: +82 63 270 3996, Fax.: +82 63 270 2472
E-mail address: csman@chonbuk.ac.kr
DOI 10.1007/s12206-007-1106-6

and combustion characteristics.

In this study, ignition and combustion tests were performed at various conditions to verify combustion behavior. At the same time, spray characteristics of the rotating fuel injection system were investigated by using laser diagnostic techniques. From these experiments, we could elucidate ignition and combustion characteristics of the slinger combustor with a rotating fuel injection system.

2. Experimental apparatus

Combustion tests were performed in the combustor test facility of KARI. Fig. 1 shows a schematic diagram of the test rig. The rotating fuel nozzle is directly linked with a high-speed electric motor located inside of the test rig. Kerosene fuel is supplied through a fuel channel and injected into the combustor by centrifugal force of the rotating nozzle. Ignition is conducted with two torches.

Fig. 2 shows the flow pattern of the combustor. The combustor is composed of an outer liner, an inner liner, a hollow guide vane and a rotating fuel nozzle. The detailed flow structures of air, fuel and combustion gas within the combustor are traced in Fig. 2.

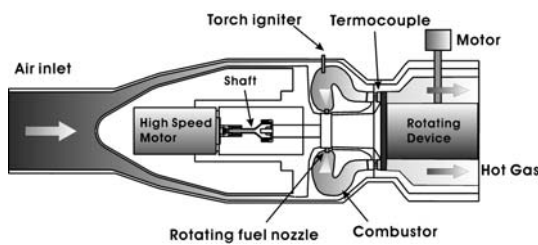


Fig. 1. Schematic diagram of combustion test rig.

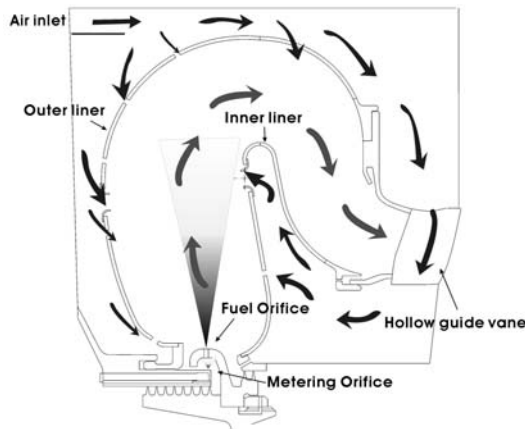


Fig. 2. Schematic of flow pattern in combustor.

Fig. 3 shows the thermocouples at the hollow guide vane. They are installed in four hollow guide vanes (five for each vane) and equally spaced. The ignition performance is measured by twenty thermocouples installed in the leading edge of the hollow guide vanes.

Fig. 4 shows the rotating device with measuring sensors. It is installed next to the hollow guide vane for measuring combustor exit gas temperature profile, total pressure and emission. It consists of an array of pressure rake, two temperature rakes and a gas sampling probe which is cooled by water. This device rotates 360 degree per 3 minutes. To calculate the combustion efficiency, concentrations of CO, CO₂, NO_x, and unburned hydrocarbon are measured from the sampling gas.

Fig. 5 shows a schematic diagram of the spray test rig. The experimental apparatus consists of a high-

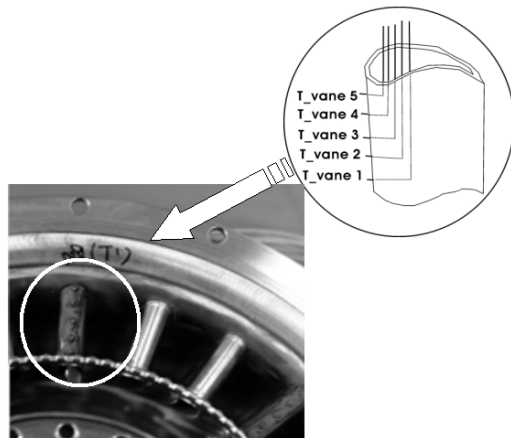


Fig. 3. Thermocouples at the hollow guide vane.

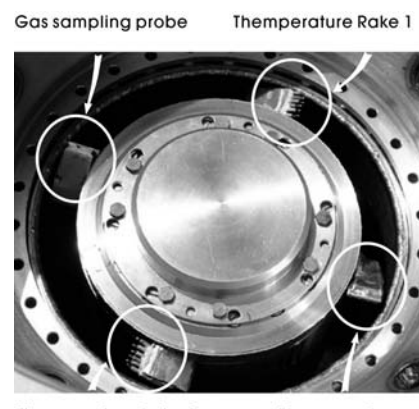


Fig. 4. Picture of the rotating device.

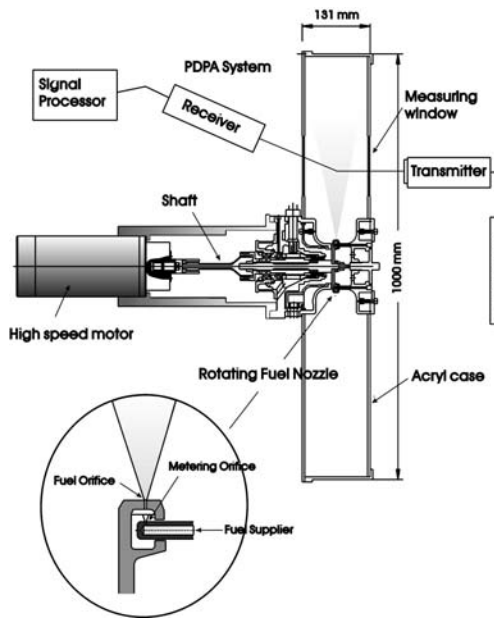


Fig. 5. Schematic diagram of spray test rig with PDPA system.

speed motor, a shaft, a rotating fuel nozzle, an acrylic case and a PDPA system. The high-speed electric motor and shaft are directly connected with the rotating fuel nozzle. The spray nozzle is placed at the center of the X and Y plane and rotates counterclockwise. The dimension of the acrylic case is a 1,000 mm(L) × 1,000 mm(H) × 131 mm(W) square box. The PDPA measurement system is composed of a laser source, a transmitter, a receiver, a signal processor and a 3D traverse system. A 5W Ar-Ion(Innova 70, Coherent Co.) laser and green and blue beam(wave length 514.5 nm and 488 nm) are used for measuring two-dimensional velocity component and droplet size. The spray visualization was performed by a digital camera with high shutter speed and pulse volume beam from 120 mJ Nd:YAG laser.

3. Experimental conditions

The ignition test was performed under ambient conditions with kerosene fuel. Fig. 5 shows a typical ignition sequence of this test. The procedure is described as follows.

- STEP 1 - Supply air to the combustor
- STEP 2 - Rotate the fuel nozzle to desired speed
- STEP 3 - Start the torch igniter
- STEP 4 - Supply fuel to the combustor
- STEP 5 - Check the ignition by gas temperature

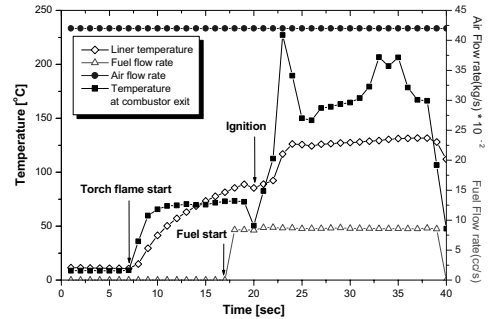


Fig. 6. Typical ignition sequence.

In Fig. 6, the gas temperature is increased by 60 °C after the torch is on, and then it is over 100 °C after successful ignition. From the preceding descriptions, ignition limits are determined by the flame gas temperature under certain fuel and air mass flow rate conditions.

To verify the effect of shaft speed, it is smoothly increased from 13,000 rpm to 30,000 rpm with constant equivalence ratio of 0.31, airflow of 1.5 kg/s, air temperature of 450 K and air pressure of 3.5 bar. To see the effect of equivalence ratio, it is increased from 0.1 to 0.3 with air flow rate of 0.6 kg/s and constant shaft speed of 13,000 rpm. To see the general performance of the slinger combustor, a combustion test was conducted at shaft speed 35,000 rpm, air temperature of 450 K and air pressure of 3.5 bar. The equivalence ratio is about 0.26. Also, combustion pressure loss was measured at various combustor inlet air speeds with air temperature 400 K, air pressure 3.5 bar and equivalence ratio of 0.26.

4. Ignition and spray test

Ignition limits are shown in Fig. 7. The data interpolation is done by cubic B-spline connection. Equivalence ratio is 0.33 at 7,300 rpm, 0.17 at 10,400 rpm and 0.15 at 13,000 rpm respectively at constant mass flow parameter of 5.0. In this result, the ignition limit is considerably increased with the shaft speed from 7,300 rpm to 10,400 rpm, but it is slightly increased with the shaft speed from 10,400 rpm to 13,000 rpm. The change of ignition limit is considered to be mainly due to the variance of droplet size distribution with the shaft speed.

The water spray test result [5] is shown in Fig. 8. The data are connected by smooth curve fitting. SMD is about 64 μm on the 5,000 rpm, 48 μm on the 10,000 rpm and 47 μm on the 20,000 rpm at the

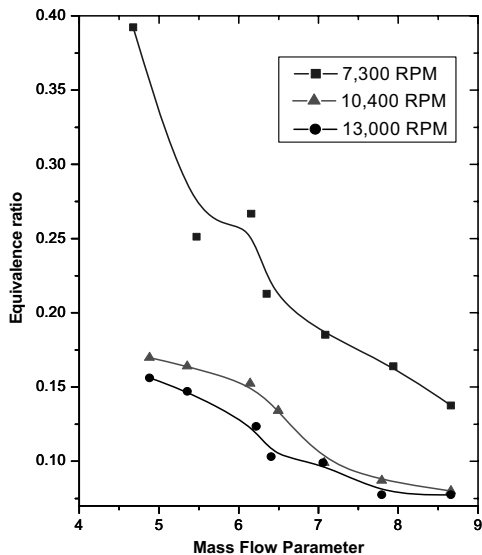


Fig. 7. Ignition limits.

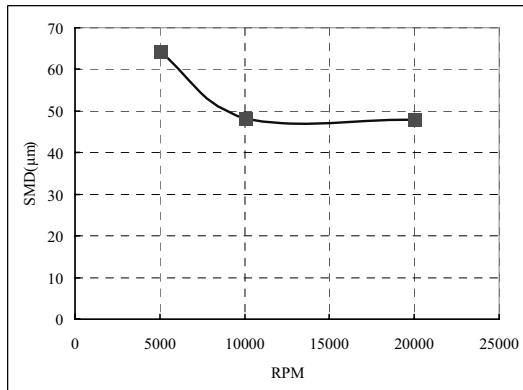


Fig. 8. Sauter mean diameter with rpm.

60 mm radial distance from rotating nozzle tip surface. The results clearly explain why ignition limits rapidly change from 7,300 to 10,400 rpm and smoothly change from 10,400 rpm to 13,000 rpm.

Fig. 9 shows the liquid breakup process at rotational speeds of 2,500, 5,000, 7,500, 10,000, 15,000 and 20,000 rpm. Dahm pointed out that the primary liquid breakup process would occur in liquid column mode or near the transition between the liquid column mode and the bag mode. [6]

From 2,500 to 5,000 rpm, the liquid film that issues from the orifice hole is drawn into a single ligament and then undergoes breakup process. This condition corresponds to “subcritical liquid breakup.” In subcritical breakup, surface tension is sufficiently strong relative to the film inertia to draw the liquid into a

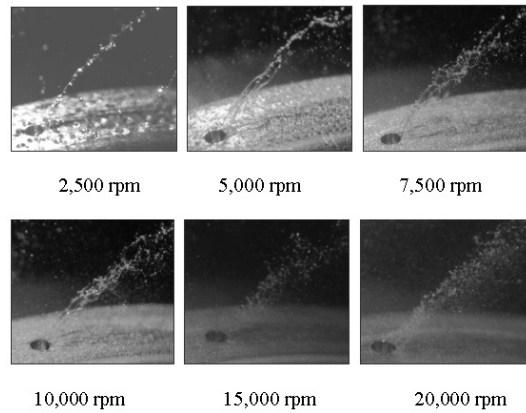


Fig. 9. Spray visualization with rotational speed.

single large ligament. From 15,000 to 20,000 rpm, the numbers of ligaments are increased and the ligament leads to fine drop sizes. This condition corresponds to “super-critical liquid breakup.” In supercritical breakup, inertial effects cause the film to break into many smaller ligaments. The transition between subcritical to supercritical phenomena can be seen in 7,500 to 10,000 rpm. So, these visualization results suggest a clear correlation with drop size and ignition performance with rotational speed.

Moreover, In Fig. 7 at 7,300 rpm, while increasing mass flow parameter from 5.0 to 8.7, the equivalence ratio varies from 0.39 to 0.13. Also at 13,000 rpm, the equivalence ratio varies from 0.16 to 0.08. It is considered that a higher mass flow parameter makes higher air velocity in the combustor, and it affects good mixing of air and fuel. In these results, ignition limits are increased with mass flow parameter in the same shaft speed condition. Consequently, there are two major factors influencing the ignition limits: shaft speed and mass flow parameter. Better ignition capability can be attained through increasing the shaft speed and the mass flow parameter.

5. Combustion test

Gas temperature was measured to determine the relationship between shaft speed and combustor exit gas temperature. Fig. 10 shows combustor exit gas temperature with shaft speed. In this test, the equivalence ratio was kept constant at about 0.32. In the range of 14,000 rpm to 16,000 rpm, gas temperature is steeply increased from 150 °C to 450 °C, and over 16,000 rpm, it is increased smoothly. However, up to 30,000 rpm, the gas temperature is flat and keeps a

constant value. This experimental result shows that combustion is directly affected by the shaft speed. According to droplet measurement results [5], it is considered that droplet size is the main factor in combustion characteristics. About the shaft speed of 15,000 rpm, there are large temperature fluctuations, and that is due to shaft vibration.

Fig. 11 shows combustion efficiency with the shaft speed. Test conditions were as follows: air flow rate of 1.5 kg/s, air pressure of 3.5 bar and air temperature of 450 K. The combustion efficiency was calculated by EI(Emission Index) method using sampling gas. The combustion efficiency is increased from 99.1% to 99.62% while the shaft speed is increased from 15,000 rpm to 30,000 rpm. Over 30,000 rpm, the combustion efficiency is not changed and kept constant. From Fig. 7 and Fig. 8, combustion efficiency could be improved by increasing the shaft speed without changing air and fuel flow rate.

Fig. 12 shows temperature profiles at the combustor exit with rotating device angle. The temperature profiles of 12 thermocouples on the rotating device have a similar pattern with the time. It means that combustion took place uniformly at every flame tube

region. That would be mainly due to the rotating fuel injection system which has a homogeneous droplet distribution like an infinite number of fuel nozzle spray.

Fig. 13 shows the pattern and profile factor of equivalence ratio 0.26. These temperature profiles were calculated by 12 thermocouple temperatures from Fig. 10. The profile looks like a bow shape and the maximum value position is about 40% turbine height. The profile factor is about 3% and this value is extremely good compared with other annular combustors using a conventional fuel injector. It could be explained that fuel is sprayed by the rotating fuel injection system uniformly and is mixed with air, and finally it makes very homogeneous fuel-air mixture at the entire flame tube region. The pattern factor is about 15% and maximum value was found at 75% turbine height. This pattern is a very good value compared with an annular combustor with air blast spray nozzle [7], and the maximum position is very desirable for turbine life.

Fig. 14 shows total pressure loss with critical Mach number for combustion and without combustion conditions. The two pressure-loss curves increase with critical Mach number. At the critical Mach number

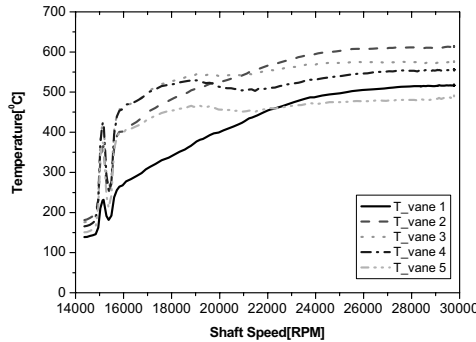


Fig. 10. Combustor exit gas temperature with shaft speed.

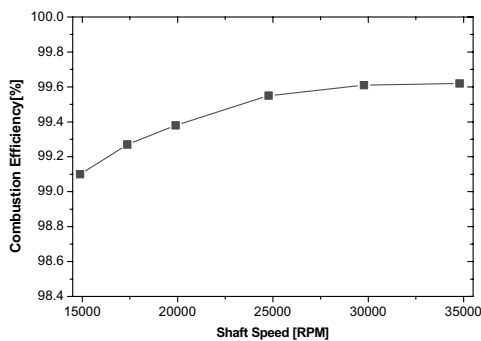


Fig. 11. Combustion efficiency with shaft speed.

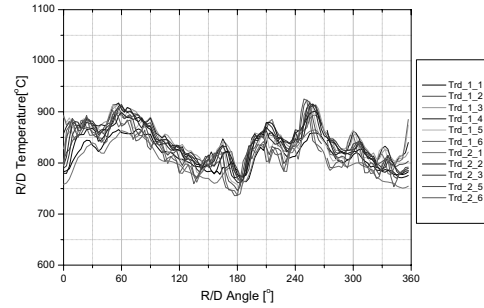


Fig. 12. Combustor exit gas temperature with rotating device angle.

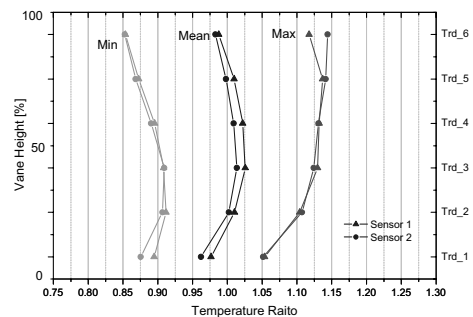


Fig. 13. Pattern and profile factor with vane height.

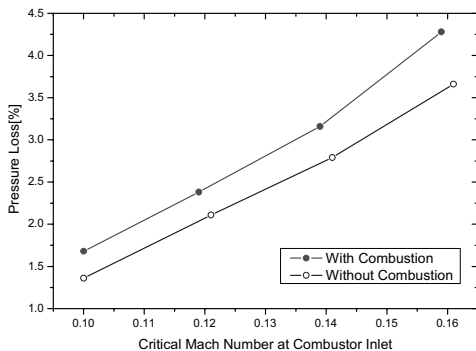


Fig. 14. Total pressure loss with critical Mach number.

0.16, pressure loss for the combustion condition is about 4.3% and cold pressure loss is about 3.6%. The relative difference of these two cases is about 16%. So this combustor aerodynamic pressure loss is about 84% and combustion pressure loss is about 16%.

6. Conclusions

The objective of this study was to understand the ignition and combustion characteristics of an annular combustor with a rotating fuel injection system.

In the ignition test, ignition limit is largely increased with the shaft speed from 7,300 rpm to 10,400 rpm, but it is only slightly increased with the shaft speed from 10,400 rpm to 13,000 rpm.

From the spray visualization, the transition between sub-critical to super-critical breakup process could be seen in 7,500 to 10,000 rpm. Also SMD is about 64 μm on the 5,000 rpm, 48 μm on the 10,000 rpm and 47 μm on the 20,000 rpm. So we find that fuel drop size is inversely proportional to the shaft speed below 10,000 rpm. However, there is almost no correlation between fuel drop size and shaft speed above 10,000 rpm, but the number of ligaments is increased and it leads to a change in the regional distribution of the fuel.

In the combustion test, the measured value for combustion efficiency is 99.6%, the pattern factor is 15%, and the profile factor is 3%. In the results, combustion efficiency can be improved by increasing shaft speed without changing the air and fuel flow rate. In the accelerating test, flame is unstable near 15,000 rpm, but the flame is very stable over 20,000 rpm. The combustor outlet temperature profile is extremely good and the maximum value position is about 75% of the turbine height. The total pressure loss is 4.3% at critical Mach number 0.16. The aero-

dynamic pressure loss is 84% and combustion pressure loss is 16% of the total pressure loss.

Nomenclature

P	: Inlet pressure [bar]
T	: Air temperature [K]
rpm	: Revolutions per minute
T_{vane}	: Combustion gas temperature at hollow guide vane
W	: Air flow rate [kg/s]
PDPA	: Phase Doppler particle analyzer
SMD	: Sauter mean diameter [μm]
Mass Flow Parameter : $W\sqrt{T}/P$	
F	: Fuel flow rate [kg/s]
A	: Air flow rate [kg/s]
Equivalence ratio :	$\phi = \frac{(F/A)_{\text{actual}}}{(F/A)_{\text{stoichiometric}}}$
$T_{\text{local,max}}$: Combustor outlet local maximum temperature [K]
T_{inlet}	: Combustor inlet temperature [K]
T_{outlet}	: Combustor outlet temperature [K]
$T_{\text{radial,max}}$: Combustor radial average maximum temperature [K]
P_{outlet}	: Combustor outlet pressure
P_{inlet}	: Combustor inlet pressure
T_{measured}	: Measured combustor outlet temperature
Pattern Factor :	$100 \times \frac{T_{\text{local,max}} - T_{\text{inlet}}}{T_{\text{outlet}} - T_{\text{inlet}}}$
Profile Factor :	$100 \times \frac{T_{\text{radial,max}} - T_{\text{inlet}}}{T_{\text{outlet}} - T_{\text{inlet}}}$
Pressure Loss :	$100 \times \frac{P_{\text{outlet}} - P_{\text{inlet}}}{P_{\text{inlet}}}$
Temperature ratio :	$\frac{T_{\text{measured}} - T_{\text{inlet}}}{T_{\text{outlet}} - T_{\text{inlet}}}$

References

- [1] NREC, The design and development of gas turbine combustors, Northern Research and Engineering Corporation, USA, (1980) 6. 32-6. 34.
- [2] A. H. Lefebvre, Atomization and Spray, Hemisphere Publishing Corporation, USA, (1989) 134-142.
- [3] H. C. Maskey, F. X. Marsh, The annular combustion chamber with centrifugal fuel injection, SAE 444C, USA, (1962)
- [4] C. Rogo, R. L. Trauth, Design of high heat release slinger combustor with rapid acceleration requirement, SAE 740167, USA, (1974).
- [5] S. Choi, K. Lee and D. Lee, J. Park, Spray charac-

- teristics of the rotating fuel injection system by using PDPA and PIV, 17th International Symposium on Air Breathing Engine, Germany, (2005) ISABE 2005-1217.
- [6] W. J. A. Dahm, P. R. Patel and B. H. Lerg, Visualization and fundamental analysis of liquid atomization by fuel slingers in small gas turbine engines, 32nd AIAA Fluid Dynamics Conference and Exhibit, USA, (2002) AIAA 2002-3183.
- [7] R. K. Mishra, P. S. Ramanujam, C. Badarinath and M. N. Bhat, Influence of operating pressure on the performance of an aero gas turbine combustor, 17th International Symposium on Air Breathing Engine, Germany, (2005) ISABE2005-1020.